



UWS Academic Portal

Floquet-Bloch analysis of analytically solvable Hill equations with continuous potentials

Caffrey, Stuart; Morozov, G. V.; MacBeath, D.; Sprung, Donald W. L.

Published in:
Journal of the Optical Society of America B

DOI:
[10.1364/JOSAB.33.001190](https://doi.org/10.1364/JOSAB.33.001190)

Published: 19/05/2016

Document Version
Peer reviewed version

[Link to publication on the UWS Academic Portal](#)

Citation for published version (APA):
Caffrey, S., Morozov, G. V., MacBeath, D., & Sprung, D. W. L. (2016). Floquet-Bloch analysis of analytically solvable Hill equations with continuous potentials. *Journal of the Optical Society of America B*, 33(6), 1190-1196. <https://doi.org/10.1364/JOSAB.33.001190>

General rights

Copyright and moral rights for the publications made accessible in the UWS Academic Portal are retained by the authors and/or other copyright owners and it is a condition of accessing publications that users recognise and abide by the legal requirements associated with these rights.

Take down policy

If you believe that this document breaches copyright please contact pure@uws.ac.uk providing details, and we will remove access to the work immediately and investigate your claim.

Floquet-Bloch Analysis of Analytically Solvable Hill Equations with Continuous Potentials

S. Caffrey and G. V. Morozov¹ and D. MacBeath and D. W. L. Sprung²

¹*Scottish Universities Physics Alliance (SUPA),
Institute of Thin Films, Sensors and Imaging,
University of the West of Scotland, Paisley, PA1 2BE, Scotland, UK*

²*Department of Physics and Astronomy, McMaster University
Hamilton, Ontario L8S 4M1 Canada*

(Dated: April 19, 2016)

Exact analytical solutions of two Hill's equations which have continuously differentiable coefficients, are obtained in terms of the Floquet-Bloch fundamental system. New features of the band structures of those equations are reported and investigated.

© 2016 Optical Society of America

OCIS codes: 050.5298, 260.2110, 000.3860

1. Introduction

Hill's differential equation

$$\frac{d^2\Psi(z)}{dz^2} + Q(z)\Psi(z) = 0, \quad Q(z) = Q(z + d), \quad (1)$$

governs the propagation of waves through a periodic system, in various physical applications *e.g.* modeling the motion of an electron in a 1D superlattice [1], or the flow of light in a one-dimensional (1D) photonic crystal [2] and in slabs with a time-periodic dielectric function [3], or the scattering properties of particles subject to a time-periodic Hamiltonian [4].

Depending on the values of the parameters involved, the solutions of Hill's equation either remain bounded for all z , or their amplitudes grow exponentially as z increases/decreases. In the first case the solutions represent allowed bands and in the second case, bandgaps. A detailed analysis of Hill's equation is provided by Floquet-Bloch theory, see Refs. [5–8]. In particular, this theory allows one to determine the band structure for any given periodic function $Q(z)$. In the case of quantum mechanics, $Q(z) = \frac{2m}{\hbar^2} [E - V(z)]$, is linearly related to the potential energy $V(z)$, so for brevity we will generally refer to $Q(z)$ as a “potential”.

For most functions $Q(z)$, Hill's equation can only be solved using numerical or approximate analytical methods. The class of exactly solvable Hill's equations includes those equations with a piecewise constant or monomial function $Q(z)$, and three cases discovered some thirty years ago, see Refs. [9–11]. The latter are a special set of equations with continuously differentiable functions

$Q(z)$. However, the exact solutions obtained in Refs. [9–11] were not sufficiently smooth (either they or their first derivatives exhibit discontinuities, which are awkward for their applications to physical problems). In Ref. [12], smooth solutions were finally obtained and analyzed for the Takayama potential [11].

The purpose of this paper is to find smooth and exact analytical solutions for the Casperson [9] and Wu-Shih [10] potentials. Then, using Floquet-Bloch theory, to obtain and analyze the band structures of those potentials. Special attention will be given to those regions of the band structure where any solution of Hill's equation becomes a periodic function.

2. Smooth Normalized Solutions for the Casperson and Wu-Shih Potentials

The periodic potential treated by Casperson in Ref. [9] has the form

$$Q_c(z) = \frac{a}{(1 + q \cos 2z)^4} + \frac{4q \cos 2z}{1 + q \cos 2z}, \quad -1 < q < 1. \quad (2)$$

The normalized solutions of Eq. (1) obtained in Ref. [9] are

$$\begin{aligned} c_1(z) &= \frac{1 + q \cos 2z}{1 + q} \cos \Phi_c(z, a, q), \\ c_2(z) &= -\frac{(1 + q)(1 + q \cos 2z)}{\sqrt{a}} \sin \Phi_c(z, a, q), \end{aligned} \quad (3)$$

where

$$\Phi_c(z, a, q) = \frac{\sqrt{a}}{2(1-q^2)} \left[\frac{q \sin 2z}{1+q \cos 2z} - \frac{2 \arctan \left(\sqrt{\frac{1-q}{1+q}} \tan z \right)}{\sqrt{1-q^2}} \right].$$

One can see that the potential $Q_c(z)$ is a continuously differentiable function, while the solutions $c_1(z)$ and $c_2(z)$ have singularities at the points $z_j = d/2 + jd$, $j = 1, 2, \dots$, where $d = \pi$ is the period of the potential $Q_c(z)$. At such points the first derivative of the function $c_1(z)$ and the function $c_2(z)$ itself have jump discontinuities.

Taking into account that the above solutions (3) are continuously differentiable on the first half of the first period, i.e for $0 \leq z < d/2$, we construct continuously

differentiable normalized solutions $u(z)$ and $v(z)$ within each period $j = 1, 2, \dots$ as follows

$$\begin{aligned} u_j(z) &= \frac{1+q \cos 2z}{1+q} \cos \Phi_c(z, a, q, j), \\ v_j(z) &= -\frac{(1+q)(1+q \cos 2z)}{\sqrt{a}} \sin \Phi_c(z, a, q, j), \end{aligned} \quad (4)$$

where

$$\Phi_c(z, a, q, j) = \frac{\sqrt{a}}{2(1-q^2)} \left[\frac{q \sin 2z}{1+q \cos 2z} - \frac{2 \left((j-1)\pi + \operatorname{arccot} \left(\sqrt{\frac{1+q}{1-q}} \cot z \right) \right)}{\sqrt{1-q^2}} \right].$$

The results are shown in Fig. 1.

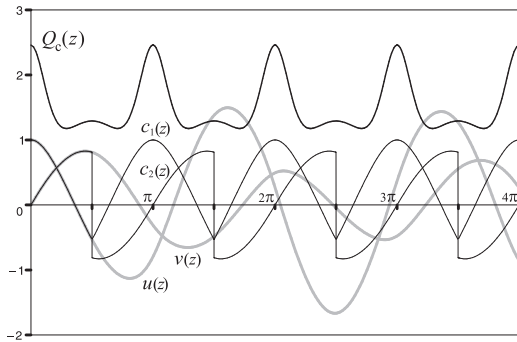


Fig. 1. Casperson potential $Q_c(z)$ (black line) and original non-smooth Casperson solutions $c_1(z)$ and $c_2(z)$ (thin black lines) compared with continuously differentiable normalized solutions $u(z)$ and $v(z)$ (thick grey lines), for $q = -0.25$ and $a = 1.20$ on the first four periods of the $Q_c(z)$.

A similar periodic potential

$$Q_w(z) = \frac{a + q^2 \sin^2 2z}{(1 + q \cos 2z)^2} + \frac{2q \cos 2z}{1 + q \cos 2z}, \quad -1 < q < 1, \quad (5)$$

was later treated in Ref. [10]. The normalized solutions of Eq. (1) obtained there have the form

$$\begin{aligned} w_1(z) &= \sqrt{\frac{1+q \cos 2z}{1+q}} \cos \Phi_w(z, a, q), \\ w_2(z) &= \operatorname{sgn}(a) \sqrt{\frac{(1+q)(1+q \cos 2z)}{a}} \sin \Phi_w(z, a, q), \end{aligned} \quad (6)$$

where

$$\Phi_w(z, a, q) = \sqrt{\frac{a}{1-q^2}} \arctan \left(\sqrt{\frac{1-q}{1+q}} \tan z \right).$$

In this paper we use the version of the step-function $\operatorname{sgn}(a)$ defined as

$$\operatorname{sgn}(a) = \begin{cases} 1, & a \geq 0, \\ -1, & a < 0. \end{cases}$$

As was the case for the potential $Q_c(z)$, the potential $Q_w(z)$ is continuously differentiable, while the solutions $w_1(z)$ and $w_2(z)$ have singularities [jump discontinuities for the first derivative of the function $w_1(z)$ and for the function $w_2(z)$ itself] at the points $z = d/2 + jd$, $j = 1, 2, \dots$, where $d = \pi$ is the period of the potential $Q_w(z)$. Again, taking into account that the solutions (6) are continuously differentiable on the first half of the first period, i.e for $0 \leq z < d/2$, we construct continuously differentiable normalized solutions $u(z)$ and $v(z)$

within each period $j = 1, 2, \dots$ as follows

$$\begin{aligned} u_j(z) &= \sqrt{\frac{1+q \cos 2z}{1+q}} \cos \Phi_w(z, a, q, j), \\ v_j(z) &= \text{sgn}(a) \sqrt{\frac{(1+q)(1+q \cos 2z)}{a}} \sin \Phi_w(z, a, q, j), \end{aligned} \quad (7)$$

where

$$\begin{aligned} \Phi_w(z, a, q, j) &= \sqrt{\frac{a}{1-q^2}} \\ &\times \left[(j-1)\pi + \text{arccot} \left(\sqrt{\frac{1+q}{1-q}} \cot z \right) \right]. \end{aligned}$$

These results are illustrated in Fig. 2.

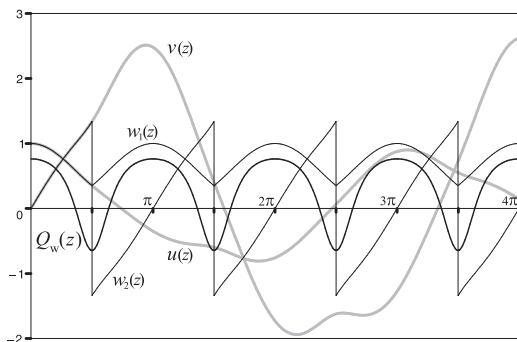


Fig. 2. Wu-Shih potential $Q_w(z)$ (black line) and the original non-smooth Wu-Shih solutions $w_1(z)$ and $w_2(z)$ (thin black lines) compared to continuously differentiable normalized solutions $u(z)$ and $v(z)$ (thick grey lines), for $q = 0.45$ and $a = 0.30$ on the first four periods of $Q_w(z)$.

We should mention that both the Caspersen and Wu-Shih potentials have a period $d = \pi$. However, all derivations in this paper remain valid for Hill's equations, with modified Caspersen and Wu-Shih potentials of arbitrary period d , $Q_{c,w}^m = \pi^2/d^2 Q_{c,w}$, provided one substitutes $z \rightarrow (\pi/d)z$.

3. Floquet-Bloch Analysis

As mentioned in the Introduction, a detailed analysis of Hill's equation is provided by Floquet-Bloch theory, which states that among the many fundamental systems of solutions of Eq. (1) there is a special one called the Floquet-Bloch system, see Refs. [5–8]. This special fundamental system contains at least one nontrivial particular solution, $F_1(z)$, of Eq. (1) with the property

$$F_1(z) = P_1(z) e^{i\xi z}, \quad P_1(z+d) = P_1(z), \quad (8)$$

where $P_1(z)$ is a periodic function of period d and ξ is the Bloch wavenumber. Such a solution is commonly referred to as a Bloch wave.

In most cases, the second solution of the Floquet-Bloch fundamental system constitutes a second Bloch wave

$$F_2(z) = P_2(z) e^{-i\xi z}, \quad P_2(z+d) = P_2(z). \quad (9)$$

One can see that both Bloch waves obey the relation

$$F_j(z+d) = \rho_j F_j(z), \quad j = 1, 2, \quad (10)$$

where the constants ρ_j are non-zero, generally complex-valued numbers, called Floquet multipliers. They satisfy the relation

$$\rho_1 \rho_2 = 1 \quad (11)$$

and are related to the Bloch wavenumber via

$$\rho_{1,2} = e^{\pm i\xi d}. \quad (12)$$

In allowed bands (regions of stability) both Bloch waves are bounded propagating functions. In the bandgaps (regions of instability) one Bloch wave decreases along the axis of propagation, while the other one grows exponentially. That growing wave is an un-physical solution in an infinite periodic structure.

On the boundaries between allowed bands and bandgaps, the two Bloch waves coincide, i.e. $F_1(z) = F_2(z) \equiv F(z)$. The constants $\rho_{1,2}$ also coincide, i.e. $\rho_1 = \rho_2 \equiv \rho$ and, in accordance with Eq. (11), either $\rho = 1$ or $\rho = -1$. In the former case the function $F(z)$ has a period d , while in the latter case it has a period $2d$. These often overlooked special cases were treated in the context of 1D superlattices in Ref. [13], and in the context of 1D photonic crystals in Refs. [14, 15]. To complete the fundamental system of Eq. (1) another particular solution is required. A common approach, see Refs. [5, 6], is to seek a second solution with the property

$$G(z) = e^{i\xi z} [zP_1(z) + P_2(z)], \quad (13)$$

which leads to

$$G(z+d) = \rho G(z) + \rho d F(z). \quad (14)$$

In this instance the function $G(z)$ is referred to as a hybrid Floquet mode.

Another case of special interest is a so-called incipient band (or vanishing gap). In that case the constants $\rho_{1,2}$ are equal, but the two Bloch waves are independent periodic functions, with the same periodicity (d if $\rho = 1$, or $2d$ if $\rho = -1$). As a result, any linear combination, $\psi(z) = C_1 F_1(z) + C_2 F_2(z)$, is also a periodic solution of Eq. (1).

A. Band Structure

Band structure analysis of a periodic potential is often carried out using the dispersion relation

$$\cos(\xi d) = \frac{u(d) + v'(d)}{2}, \quad (15)$$

where the functions $u(z)$ and $v(z)$ are continuously differentiable normalized solutions. Thus, for a real valued potential $Q(z)$ the function $\cos(\xi d)$ is also real and satisfies the relation $-1 < \cos(\xi d) < 1$ in allowed bands and $|\cos(\xi d)| > 1$ in bandgaps.

A well-known physical example of a periodic system is a 1D photonic crystal, with the refractive index $n(z) = n(z + d)$. Let an optical wave of wavenumber $k = \omega/c$, where ω is the angular frequency of light and c is the light velocity in vacuum, impinge on the crystal at angle θ_{in} . The light is s -polarized when the electric field is normal to the plane of incidence and is p -polarized when the electric field lies in the plane of incidence. With the aid of a parameter β , which is related to the refractive index of the incident medium n_{in} and the incident angle θ_{in} as $\beta = kn_{\text{in}} \sin \theta_{\text{in}}$, the periodic potential $Q(z)$ in Eq. (1) for such a problem takes the form

$$\begin{aligned} Q_{\text{TE}}(z) &= k^2 n^2(z) - \beta^2, \\ Q_{\text{TM}}(z) &= k^2 n^2(z) - \beta^2 + \frac{1}{n(z)} \frac{d^2 n}{dz^2} - \frac{2}{n^2(z)} \left(\frac{dn}{dz} \right)^2 \end{aligned} \quad (16)$$

for TE and TM polarizations respectively.

The function $\Psi(z)$ in Eq. (1) becomes the electric field for TE polarized light, or the magnetic field divided by $n(z)$ for TM polarized light. The simplest 1D photonic crystal is a binary crystal, formed by homogeneous alternating layers of two low-loss dielectrics, as illustrated in Fig. 3.

For a binary crystal the functions $u(z)$ and $v(z)$ can easily be found analytically, see Refs. [14, 15]. The band structure of a typical crystal is shown in Fig. 4. One can see there examples of all the aforementioned features of band structure, including incipient bands.

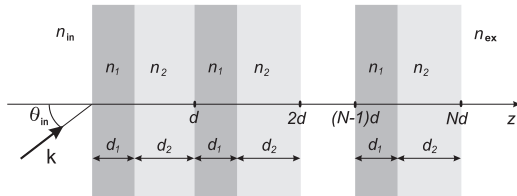


Fig. 3. Optical wave incident on a binary photonic crystal $\{n_1 n_2\}^N$; n_1 and n_2 are the refractive indices of two dielectric layers with thicknesses d_1 and d_2 ; N is the number of periods, n_{in} and n_{ex} are the refractive indices of the incident and exit media.

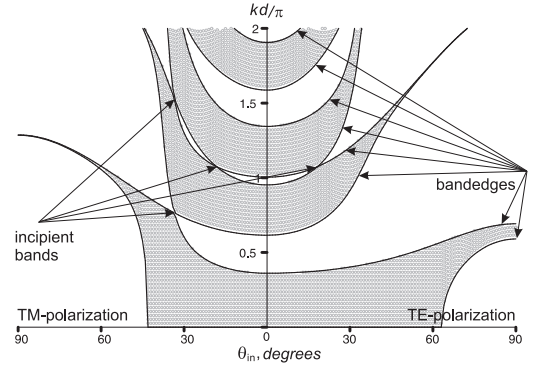


Fig. 4. Band structure of a binary photonic crystal, see Fig. 3, with $n_1 = 1.5$, $n_2 = 3.5$, $d_1 = 40$ nm, $d_2 = 15$ nm. The refractive index of the incident medium is $n_{\text{in}} = 2.5$. The allowed bands are shown in grey background, the bandgaps are shown in white.

The band structure analysis based on the dispersion relation (15) covers various physical periodic system including single-negative (permittivity- or permeability-negative) materials, see Ref. [16]. Using that relation with $u(z)$ and $v(z)$ given by Eq. (4) or Eq. (7), respectively, we now calculate the band structures of the Casperson and Wu-Shih potentials. For those potentials one has $\cos(\xi d) = u(d) = v'(d)$ which leads to

$$\begin{aligned} \cos(\xi d) &= \cos \left[\pi \sqrt{\frac{a}{(1-q^2)^3}} \right] \quad (\text{Casperson}), \\ \cos(\xi d) &= \cos \left[\pi \sqrt{\frac{a}{1-q^2}} \right] \quad (\text{Wu - Shih}). \end{aligned} \quad (17)$$

Both these potentials have unusual band structures with a bandedge at $a = 0$ separating a single allowed band ($a > 0$) from a single bandgap ($a < 0$). Their incipient bands are given by

$$\begin{aligned} \frac{a}{(1-q^2)^3} &= m^2, \quad m = 1, 2, 3, \dots \quad (\text{Casperson}), \\ \frac{a}{1-q^2} &= m^2, \quad m = 1, 2, 3, \dots \quad (\text{Wu - Shih}). \end{aligned} \quad (18)$$

In addition, each potential has an additional incipient band at $a > 0$ in the degenerate case $q = 0$. As one can see, all incipient bands of these two potentials are lines rather than single points (as seen in a binary crystal). The results are illustrated in Fig. 5 and Fig. 6.

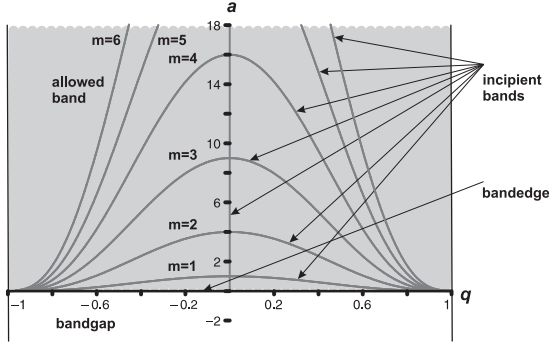


Fig. 5. Band structure of the Casperson potential. The allowed band is shown in grey background, the bandgap is shown in white. The nondegenerate incipient bands (dark grey lines) are defined by the equation $a/(1-q^2)^3 = m^2$, $a > 0$; only the first six bands ($m = 1, 2, 3, 4, 5, 6$) are shown. The degenerate incipient band is defined by the equation $q = 0$, $a > 0$.

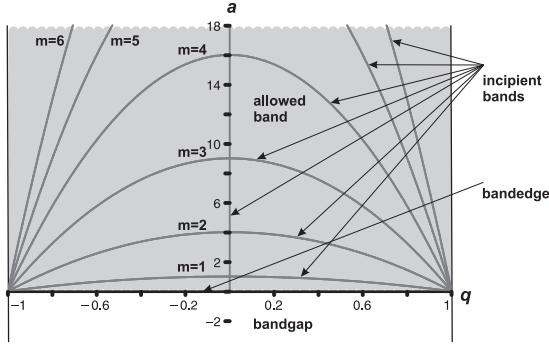


Fig. 6. Band structure of the Wu potential. The allowed band is shown in grey background, the bandgap is shown in white. The nondegenerate incipient bands (dark grey lines) are defined by the equation $a/(1-q^2) = m^2$, $a > 0$; only the first six bands ($m = 1, 2, 3, 4, 5, 6$) are shown. The degenerate incipient band is defined by the equation $q = 0$, $a > 0$.

B. Floquet-Bloch System for Allowed Bands and Bandgaps

In the allowed bands and bandgaps the Floquet-Bloch fundamental system consists of the two independent Bloch waves which are expressed in terms of the normalized solutions, see Refs. [12, 14, 15], as follows:

$$F_{1,2}(z) = u(z) + \frac{\rho_{1,2} - u(d)}{v(d)} v(z), \quad v(d) \neq 0. \quad (19)$$

For the potentials at hand

$$\begin{aligned} v(d) &= \frac{(1+q)^2}{\sqrt{a}} \sin \left[\pi \sqrt{\frac{a}{(1-q^2)^3}} \right] \quad (\text{Casperson}), \\ v(d) &= \frac{1+q}{\sqrt{a}} \sin \left[\pi \sqrt{\frac{a}{1-q^2}} \right] \quad (\text{Wu - Shih}), \end{aligned} \quad (20)$$

i.e. $v(z)$ has a node at $z = d$ only in the case of an incipient band of the above potentials, see Eqs. (17, 18). Subsequently, one can safely use Eq. (19) to build the Floquet-Bloch fundamental system in the allowed bands and bandgaps of either potential.

At this point it is worth noting that in principle it is sufficient to obtain $u(z)$ and $v(z)$ on the first period only, i.e. for $0 < z < d$. Then, due to the property

$$F_{1,2}(z + jd) = \rho_{1,2}^j F_{1,2}, \quad j = 1, 2, \dots, \quad (21)$$

it is possible to extend $F_{1,2}(z)$ throughout the entire periodic potential using Eq. (19) on the first period only.

As one should expect, the form of the Floquet-Bloch solutions is markedly different in allowed bands as compared to bandgaps. In the allowed bands they are complex-valued functions with oscillating non-periodic real and imaginary parts, related by $\Re[F_1(z)] = \Re[F_2(z)]$ and $\Im[F_2(z)] = -\Im[F_1(z)]$, see Fig. 7 and Fig. 8.

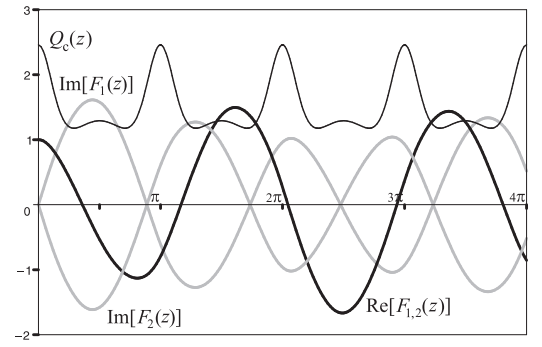


Fig. 7. Floquet-Bloch waves $F_1(z)$ and $F_2(z)$ in the allowed band of the Casperson potential $Q_c(z)$ (black line) for $q = -0.25$ and $a = 1.20$. The real parts, $\Re[F_1(z)] = \Re[F_2(z)]$, are shown by a thick black line and imaginary parts, $\Im[F_2(z)] = -\Im[F_1(z)]$, are shown by thick grey lines. Note that $\Re[F_{1,2}(z)] = u(z)$.

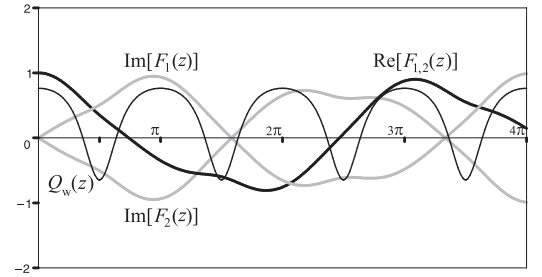


Fig. 8. Floquet-Bloch waves $F_1(z)$ and $F_2(z)$ in the allowed band of the Wu potential $Q_w(z)$ (black line) for $q = 0.45$ and $a = 0.3$. The real parts, $\Re[F_1(z)] = \Re[F_2(z)]$, are shown by a thick black line and imaginary parts, $\Im[F_2(z)] = -\Im[F_1(z)]$, are shown by thick grey lines. Note that $\Re[F_{1,2}(z)] = u(z)$.

This is in stark contrast to the form of the Floquet-Bloch solutions in the bandgaps, where both are real

functions, with one being rapidly suppressed along the axis of propagation whilst the other one is rapidly diverging, see Fig. 9 and Fig. 10.

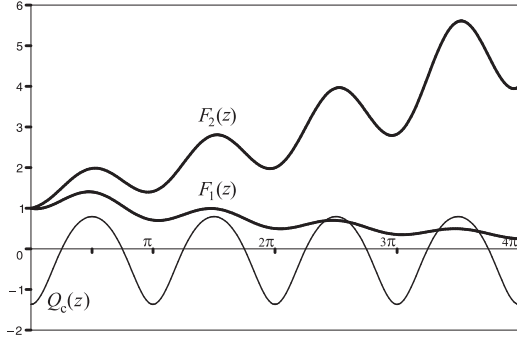


Fig. 9. Floquet-Bloch waves $F_1(z)$ and $F_2(z)$ in the bandgap of the Casperson potential $Q_c(z)$ for $q = -0.25$ and $a = -0.01$.

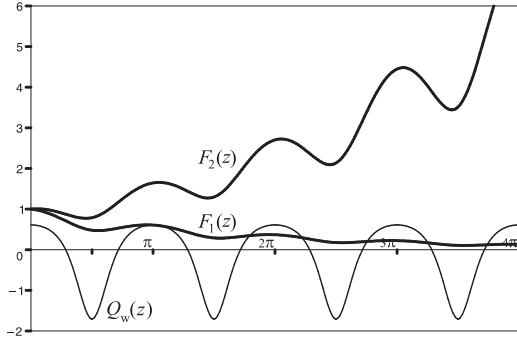


Fig. 10. Floquet-Bloch waves $F_1(z)$ and $F_2(z)$ in the bandgap of the Wu-Shih potential $Q_w(z)$ for $q = 0.45$ and $a = -0.02$.

C. Floquet-Bloch System at Bandedge Boundaries

Bandedge boundaries present a case of special interest as at such points $\rho_1 = \rho_2 \equiv \rho$ so that $F_1(z) \equiv F_2(z) \equiv F(z)$, see Eq. (19). Then, the hybrid Floquet mode $G(z)$ of Eq. (13) is required to complete the fundamental system. In terms of the normalized solutions, $u(z)$ and $v(z)$, for the case $v(d) \neq 0$, we find, see Refs. [12, 14, 15],

$$G(z) = \frac{\rho d}{v(d)} v(z), \quad (22)$$

where in accordance with Eq. (11), either $\rho = 1$ or $\rho = -1$. Subsequently, see Eq. 21, the Floquet-Bloch wave $F(z)$ becomes periodic with periodicity d for $\rho = 1$ or $2d$ for $\rho = -1$.

The only bandedge boundary for either potential occurs when $a = 0$, see Section 3.1; then $\rho_1 \equiv \rho_2 \equiv \rho = u(d) = v'(d) = 1$, and the periodic Floquet-Bloch wave $F(z)$ coincides with the normalized solution $u(z)$

$$\begin{aligned} F(z) = u(z) &= \frac{1 + q \cos(2z)}{1 + q} \quad (\text{Casperson}), \\ F(z) = u(z) &= \sqrt{\frac{1 + q \cos(2z)}{1 + q}} \quad (\text{Wu - Shih}). \end{aligned} \quad (23)$$

The second normalized solution $v(z)$ is obtained by taking the limit $a \rightarrow 0$ in Eq. (4) or Eq. (7) correspondingly. As a result, the function $v(z)$ within each period $j = 1, 2, \dots$ takes the form

$$\begin{aligned} v_j(z) &= -\frac{1}{2} \frac{q \sin 2z}{1 - q} + \frac{(1 + q \cos 2z)}{(1 - q)\sqrt{1 - q^2}} \left[(j - 1)\pi + \operatorname{arccot} \left(\sqrt{\frac{1 + q}{1 - q}} \cot z \right) \right] \quad (\text{Casperson}), \\ v_j(z) &= \sqrt{\frac{1 + q \cos 2z}{1 - q}} \left[(j - 1)\pi + \operatorname{arccot} \left(\sqrt{\frac{1 + q}{1 - q}} \cot z \right) \right] \quad (\text{Wu - Shih}). \end{aligned} \quad (24)$$

The hybrid Floquet mode $G(z)$ is defined by Eq. (22), where in accordance with Eq. (24),

$$\begin{aligned} v(d) &= \frac{\pi}{1 - q} \sqrt{\frac{1 + q}{1 - q}} \quad (\text{Casperson}), \\ v(d) &= \pi \sqrt{\frac{1 + q}{1 - q}} \quad (\text{Wu - Shih}). \end{aligned} \quad (25)$$

The results are illustrated in Fig. 11 and Fig. 12.

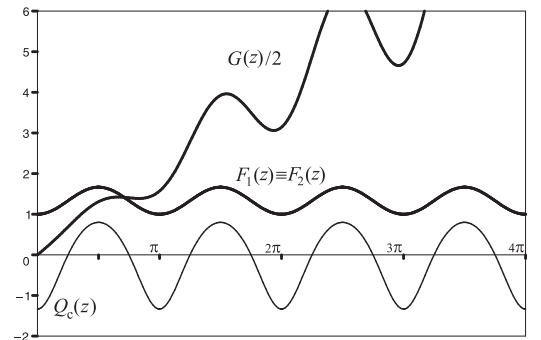


Fig. 11. Periodic Floquet-Bloch wave $F_1(z) \equiv F_2(z) \equiv F(z)$ and a hybrid Floquet mode $G(z)$ at the boundary ($a = 0$) between the allowed band and bandgap of the Casperson potential $Q_c(z)$ for $q = -0.25$.

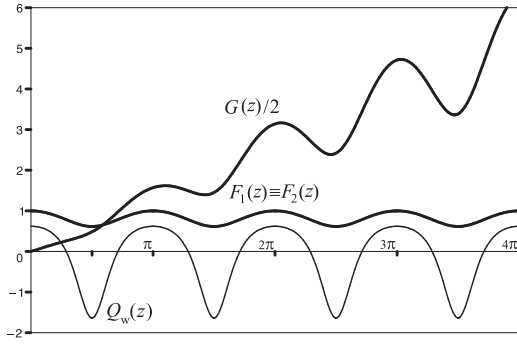


Fig. 12. Periodic Floquet-Bloch wave $F_1(z) \equiv F_2(z) \equiv F(z)$ and a hybrid Floquet mode $G(z)$ at the boundary ($a = 0$) between the allowed band and bandgap of the Wu-Shih potential $Q_w(z)$ for $q = 0.45$.

D. Floquet-Bloch System for Incipient Bands

Incipient bands provide another case of special interest as they support two periodic linearly-independent Bloch

waves, which coincide with the normalized solutions $u(z)$ and $v(z)$, see Refs. [12, 14, 15]. In these regions, as with bandedge boundaries, $\rho_1 = \rho_2 \equiv \rho$, and the periodicity of the Bloch waves depends on the value of the Floquet multiplier (d if $\rho = 1$, $2d$ if $\rho = -1$). The incipient bands (vanishing gaps) of some physical periodic systems have been studied in Refs. [17, 18].

Using the relationship, see Eqs. (18), between the parameters a and q in the incipient bands $m = 1, 2, \dots$ of the Caspersen and Wu-Shih potentials, we obtain the analytical expressions for the periodic Bloch waves within each period $j = 1, 2, \dots$ of the Caspersen potential as

$$\begin{aligned} F_{1,j}(z) &= \frac{1 + q \cos 2z}{1 + q} \cos \Phi_c^m(z, a, q, j), \\ F_{2,j}(z) &= -\frac{1 + q \cos 2z}{m(1 - q)\sqrt{1 - q^2}} \sin \Phi_c^m(z, a, q, j), \end{aligned} \quad (26)$$

where

$$\Phi_c^m(z, q, j) = m \left[\frac{q \sqrt{1 - q^2} \sin 2z}{2(1 + q \cos 2z)} - (j - 1)\pi - \operatorname{arccot} \left(\sqrt{\frac{1 + q}{1 - q}} \cot z \right) \right],$$

and within each period $j = 1, 2, \dots$ of the Wu-Shih potential as

$$\begin{aligned} F_1(z) &= \sqrt{\frac{1 + q \cos 2z}{1 + q}} \cos \Phi_w^m(z, a, q, j), \\ F_2(z) &= \frac{1}{m} \sqrt{\frac{1 + q \cos 2z}{1 - q}} \sin \Phi_w^m(z, a, q, j), \end{aligned} \quad (27)$$

where

$$\Phi_w^m(z, q, j) = m \left[(j - 1)\pi + \operatorname{arccot} \left(\sqrt{\frac{1 + q}{1 - q}} \cot z \right) \right].$$

In Fig. 13 the periodic Floquet-Bloch waves with the period $d = 2\pi$ ($\rho_1 = \rho_2 = -1$) are shown in the third incipient band ($m = 3$) of the Caspersen potential for $q = -0.25$.

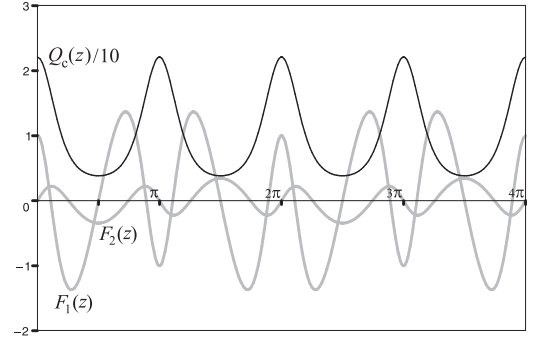


Fig. 13. Periodic Floquet-Bloch waves $F_1(z)$ and $F_2(z)$ in the third incipient band ($m = 3$) of the Caspersen potential for $q = -0.25$.

In Fig. 14 the periodic Floquet-Bloch waves with the period $d = \pi$ ($\rho_1 = \rho_2 = 1$) are shown in the fourth incipient band ($m = 4$) of the Wu-Shih potential for $q = 0.45$.

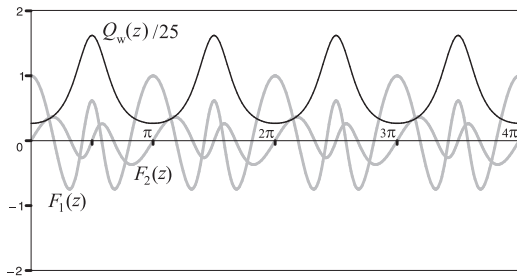


Fig. 14. Periodic Floquet-Bloch waves $F_1(z)$ and $F_2(z)$ in the fourth incipient band ($m = 4$) of the Wu-Shih potential for $q = 0.45$.

In the degenerate incipient band, $q = 0$ ($a > 0$), of both potentials, the two periodic Bloch waves reduce to

$$u(z) = \cos(\sqrt{a}z), \quad v(z) = \frac{\sin(\sqrt{a}z)}{\sqrt{a}}. \quad (28)$$

4. Conclusion

Two analytically solvable Hill's equations with continuous potentials were investigated, using the Floquet-Bloch method. In particular, the allowed bands and bandgaps of those potentials were obtained by analysis of the exact dispersion equation for the Bloch phase. The band structure of either potential is shown to possess a band-edge boundary separating a single bandgap from an allowed band, the latter divided into pieces by incipient bands (vanishing gaps). Those incipient bands are continuous second-order curves and thus they provide an example of a new kind of incipient band for a periodic potential (to date, incipient bands were reported only in the form of points or in the form of straight lines). The Floquet-Bloch solutions within each of the identified regions of band structure were then constructed and analyzed. **Certainly, to fabricate in practice photonic crystals or semiconductor superlattices with the described incipient bands is hardly achievable. However, our analysis concerning the incipient bands could explain anomalously narrow bandgaps should they be found in similar structures.** Overall, the results add to a better understanding of Floquet-Bloch theory and may provide further insight into the behavior of light within photonic crystals, or electrons in semiconductor superlattices.

5. Acknowledgements

DWLS and DM are grateful to NSERC Canada for financial support under discovery grant RGPIN-3198.

References

- [1] R. de L. Kronig and W. G. Penney, "Quantum Mechanics of Electrons in Crystall Lattices," *Proc. R. Soc. London A* **130**, 499–513 (1931).
- [2] I. Nusinsky and A. A. Hardy, "Band-gap analysis of one-dimensional photonic crystals and conditions for gap closing," *Phys. Rev. B* **73**, 125104 (2006).
- [3] J. R. Zurita-Sanchez, P. Halevi and J. C. Cervantes-Gonzalez, "Reflection and transmission of a wave incident on a slab with a time-periodic dielectric function $\varepsilon(t)$," *Phys. Rev. A* **79**, 053821 (2009).
- [4] T. Bilitewski and N. R. Cooper, "Scattering theory for Floquet-Bloch states," *Phys. Rev. A* **91**, 033601 (2015).
- [5] J. J. Stoker, *Nonlinear Vibrations* (Waverly Press, New York, 1950).
- [6] V. A. Yakubovich and V. M. Starzhinskii, *Linear Differential Equations with Periodic Coefficients* (Wiley, New York, 1975).
- [7] M. S. P. Eastham, *The Spectral Theory of Periodic Differential Equations* (Scottish Academic Press, Edinburgh, 1975).
- [8] W. Magnus and S. Winkler, *Hill's Equation* (Dover, New York, 2004).
- [9] L. W. Casperson, "Solvable Hill equation," *Phys. Rev. A* **30**, 2749–2751 (1984); Erratum: *ibid.* **31**, 2743(E) (1985).
- [10] S. M. Wu and C. C. Shih, "Construction of Solvable Hill Equations," *Phys. Rev. A* **32**, 3736–3738 (1985).
- [11] K. Takayama, "Note on solvable Hill equations," *Phys. Rev. A* **34**, 4408–4410 (1986).
- [12] G. V. Morozov and D. W. L. Sprung, "Band structure analysis of an analytically solvable Hill equation with continuous potential," *J. Opt.* **17**, 035607 (2015).
- [13] A. A. Cottey, "Floquet's Theorem and Band Theory in One Dimension," *Am. J. Phys.* **39**, 1235 (1971).
- [14] G. V. Morozov and D. W. L. Sprung, "Floquet-Bloch Waves in One-Dimensional Photonic Crystals," *EPL* **96**, 54005 (2011).
- [15] G. V. Morozov and D. W. L. Sprung, "Transverse-magnetic-polarized Floquet-Bloch Waves in One-Dimensional Photonic Crystals," *J. Opt. Soc. Am. B* **29**, 3231–9 (2012).
- [16] Y. Chen, "Unusual transmission bands of one-dimensional photonic crystals containing single-negative materials," *Opt. Express* **17**, 20333–41 (2009).
- [17] A. I. Mogilner and P. D. Loly "Vanishing gaps in 1D bandstructures," *J. Phys. A: Math. Gen.* **25**, L855–60 (1992).
- [18] H. Zhang, X. Chen, Y. Li, Y. Fu, and N. Yuan "Bragg gap vanishing phenomena in one-dimensional photonic crystals," *Opt. Express* **17**, 7800–06 (2009).